

Electron-impact excitation cross sections for the $b^3\Sigma_u^+$ state of H_2

M. A. Khakoo,* S. Trajmar, R. McAdams,[†] and T. W. Shyn[‡]

Jet Propulsion Laboratory, California Institute of Technology, Pasadena, California 91109

(Received 2 November 1984; revised manuscript received 22 September 1986)

Differential and integral cross sections for electron-impact excitation of the $b^3\Sigma_u^+$ state of H_2 have been determined in the 20–100-eV impact energy region. The calibration of the cross sections was achieved through the H_2 elastic scattering cross sections, which in turn were normalized to absolute He elastic scattering cross sections. Comparison is made with available experimental data and with theoretical results applying Born-Ochkur-Rudge, distorted-wave, and close-coupling approximations.

I. INTRODUCTION

H_2 is abundant in astrophysical and planetary environments and is the most easily amenable to theoretical treatment of all molecules. On this basis, one would expect that substantial information is available on electron-impact excitation of the various electronic states of H_2 . The fact, however, is that only fragmentary cross-section data are available even for the most extensively studied $b^3\Sigma_u^+$ state.

Electron-impact dissociation of H_2 into H atoms was studied by Corrigan.¹ His results essentially represent the sum of integral cross sections for exciting the triplet states of the molecule. The excitation of the $b^3\Sigma_u^+$ level leads directly to dissociation, while the higher triplet levels cascade down to the $b^3\Sigma_u^+$ level and dissociate through it. This dissociation cross section, therefore, represents the upper limit for the electron-impact excitation cross section of the $b^3\Sigma_u^+$ level.

Electron-impact excitation of the $b^3\Sigma_u^+$ state of H_2 was studied by Weingartshofer *et al.*² in the 10–15-eV impact energy range. They found, at an energy loss of 10.47 eV and 70° scattering angle, that the nonresonant part of the differential excitation function peaked at around 11.5-eV impact energy and that resonance contribution peaks occurred at impact energies which corresponded to the “series I” Feshbach resonances associated with a bound $2\Sigma_g^+$ state (11–12-eV region). Very recently Hall and Andric³ studied the differential excitation functions for the $b^3\Sigma_u^+$ state at impact energies from 0.2 to 2.2 eV above threshold for a 10.0-eV energy-loss value at fixed scattering angles ranging from 20° to 120° with the aim of observing the $B^2\Sigma_g^+$ core-excited shape resonance in this channel. They found no such contribution and concluded that the differential cross sections (DCS) were dominated by direct scattering. They found the differential excitation functions to be nearly constant (within $\pm 20\%$) at 10.5-, 11-, and 12-eV impact energies (for their 10.0-eV energy-loss channel) at all angles. This is not in contradiction with the results of Weingartshofer *et al.*² since the peak value in their 70° DCS at 11.5 eV was only 10% above the average values in the 10–12-eV region. At higher impact energies ($E_0 = 25$ –60 eV) Trajmar *et al.*⁴ reported experimental and calculated (Ochkur-Rudge model) differential cross sections in the 10°–80° angular

range. The experimental cross sections were normalized to the theoretical results and the errors associated with the relative DCS were estimated to be about 25%. Very recently Nishimura⁵ measured differential cross sections for the $b^3\Sigma_u^+$ excitation at impact energies ranging from 13 to 60 eV. He normalized the b -state cross sections against the elastic cross sections which in turn were normalized against He by the relative flow technique.

In the present paper we report normalized experimental differential and integral cross sections for the $X^1\Sigma_g^+ \rightarrow b^3\Sigma_u^+$ excitation process by electrons in the 20–100-eV impact energy and 10°–120° angular ranges. The conversion of the measured inelastic scattering intensities into cross sections was achieved by determining the inelastic to elastic scattering intensity ratios in H_2 at fixed impact energies and scattering angles and by utilizing the differential elastic scattering cross sections of Khakoo and Trajmar.⁶ The experimental results are compared with Born-Ochkur-Rudge-type,^{7,8} distorted-wave,^{9,10} and close-coupling^{11–13} calculations. Other recent close-coupling calculations by Baluja *et al.*¹⁴ and Schneider and Collins¹⁵ yield cross sections in good agreement with Lima *et al.*¹³

II. EXPERIMENTAL PROCEDURE

In this experiment a monoenergetic beam of electrons is focused onto a target molecular beam. The scattered electrons are detected by an analyzer as a function of their kinetic energy for various selected values of scattering angles and impact energies. The electron-impact spectrometer utilized in this work was the same as for the elastic scattering measurements⁶ and was described in more detail earlier.¹⁶

The electron spectrometer employed hemispherical dispersers with virtual apertures and was capable of operating with an energy resolution of 40 meV and with a few nanoampere electron-beam current. Since the $b^3\Sigma_u^+$ energy-loss spectrum is broad and structureless, its study did not require high resolution. The apparatus, therefore, was operated with a 20-nA electron-beam current and an energy resolution of 80 meV [full width at half maximum (FWHM)]. The angular acceptance of the analyzer was approximately $\pm 5^\circ$. The angular range covered by the analyzer was -30° to 120° and the scattering angle was

accurately read to within $\pm \frac{1}{2}^\circ$ by means of a calibrated potentiometer sensitive to the angular position of the analyzer.

The target-gas beam of H_2 was generated by a multi-capillary array operated typically with 8 torr of H_2 behind the capillary array to provide a target-gas density of 10^{13} molecules cm^{-3} on the beam axis at the collision region. The collision region was located at a distance of 3 mm above the tip of the gas source. The purity of H_2 used was 99.95%.

The whole experimental apparatus was enclosed by a double μ -metal shield which reduced the magnetic fields inside the experiment to less than 10 mG. The vacuum chamber in which this was housed was pumped down typically to less than 1×10^{-7} torr and, with the gas source operating, rose to 6×10^{-6} torr. Acquisition times for obtaining energy-loss spectra of the $X \rightarrow b$ transition in H_2 varied from 2 to 8 h in this experiment.

A typical energy-loss spectrum is shown in Fig. 1. In all cases the elastically scattered electron peak was scanned first followed by a jump to the region containing the continuum. The spectra were acquired by repetitive scanning with a multichannel scaler (1024 channels with a dwell time of 0.1 seconds per channel) which also provided the ramp voltage to the electron detector. The data were then transferred to a microcomputer for unfolding and evaluation.

Since the ratios of the scattering intensities associated with the $X \rightarrow b$ continuum and elastic peak were the subject of the measurements, it was important to ensure that the energy-loss spectra were not influenced by a change in the transmission of the analyzer as a function of the energy-loss value. The analyzer was tuned to optimize both the elastic and inelastic features simultaneously. The design and the operation of the lens system of the detector incorporated an energy-adder lens and two variable-focal-length lenses to insure the same efficiency of detection for electrons from a few electron volts to a few tens of electron volts residual energy. The method was tested using

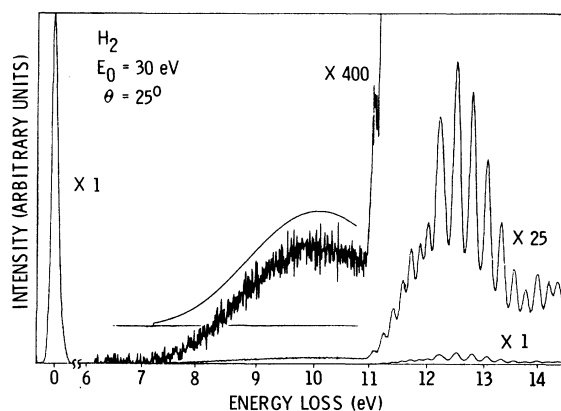


FIG. 1. Energy-loss spectrum at 30-eV impact energy and 25° scattering angle showing the elastic peak, the $b^3\Sigma_u^+$ continuum plus fitted $b^3\Sigma_u^+$ profile (offset for clarity), and the conglomeration of features associated with excitation of the discrete electronic states in H_2 .

the $\text{He } 1^1S \rightarrow 2^1P$ energy-loss and elastic scattering features and successfully reproducing the inelastic to elastic scattering intensity ratios given by the previously measured cross sections.^{17,18} At impact energies below 20 eV, a special calibration technique is required to establish the proper response function of the detector. Such a procedure is being developed and applied to near-threshold impact-energy cross-section measurements in our laboratory.

III. RESULTS, ANALYSIS, AND DISCUSSION

Electron-impact energy-loss spectra similar to those in Fig. 1 were taken at 20-, 30-, 40-, and 100-eV impact energies for scattering angles in the range of 10° – 120° . The measurements were repeated several times, in some cases after the apparatus was disassembled and cleaned, to check reproducibility.

The elastic peak intensity was determined by integrating the counts under this feature and subtracting the background counts determined in an energy-loss region well clear of elastic signal. The intensity of the $X \rightarrow b$ continuum was more difficult to determine since the continuum merges into other inelastic features of the H_2 spectrum at the energy-loss value of 11 eV and greater. Hence, to determine its intensity, the uncontaminated region of the $X \rightarrow b$ continuum in the region of 6 to 10.5 eV was fitted by a gradient search method of nonlinear least squares¹⁹ to an analytical Franck-Condon envelope calculated by Gibson.²⁰ The resulting function in turn was used to generate the continuum feature in the overlapping region. The overall feature was integrated in the energy-loss limits of 6 to 15 eV which effectively enclosed the whole transition ($\pm 0.01\%$).

The continuum Franck-Condon envelope computed by Gibson is based on the potential curve for the H_2 b state which was obtained by Kolos and Wolniewicz²¹ to determine the continuum vibrational eigenfunctions. These vibrational eigenfunctions were then integrated with the H_2 ground-state $X(v=0)$ wave function (also computed in the same way) to generate the usual overlap integrals (Franck-Condon factors) as a function of nuclear momentum k of the excited b state. The shape of this envelope was found to be in excellent agreement with the shape of the $X \rightarrow b$ continuum measured in this experiment. This normalized Franck-Condon envelope for the $X(v=0) \rightarrow b$ transition is

$$F(k) = 0.191 \exp \left[- \left(\frac{k - 19.65}{2.95} \right)^2 \right], \quad (1)$$

where k (a.u.), the nuclear momentum, is given by

$$k = \left[\frac{E - 4.478}{R} \frac{m_p}{m_e} \right]^{1/2}. \quad (2)$$

Here $R = 27.2$ eV, E (eV) is the energy-loss value of the continuum of interest, and m_p and m_e are the rest masses of the proton and electron in the same units. The value 4.478 (eV) corresponds to the dissociative threshold energy of the $b^3\Sigma_u^+$ state. The above function plus a linear background was used to fit the continuum feature. The

TABLE I. Differential cross sections for the electron-impact excitation of the $b^3\Sigma_u^+$ state of H_2 .

Scattering angle (deg)	Differential cross sections (10^{-18} cm ² /sr)			
	Impact energy (eV)			
	20	30	40	100
15		1.98	1.52	
20		1.98	1.65	
25	6.25	1.82	1.71	0.34
30	5.72	1.88	1.52	0.27
35	5.26			
40	4.87	1.98	1.33	0.19
45	4.13			
50	3.82	1.60	1.07	0.092
55				
60	3.44	1.30	0.84	0.049
65				
70	3.36	1.12	0.66	0.026
75				
80	3.27	0.99	0.54	0.013
85	3.49			
90	3.49	0.93	0.40	0.0075
95		0.91		
100	3.85	0.84	0.32	0.0051
105				
110	3.68	0.75	0.30	0.0037
115				
120	3.71	0.83	0.27	0.0031
Experimental error	11.5%	11.3%	12.9%	14.5%
Elastic error	11.0%	13.0%	14.0%	15.0%
Transmission error	10.0%	10.0%	10.0%	10.0%
Total error	18.8%	19.9%	21.5%	23.1%

TABLE II. Summary of integral cross sections for the electron-impact excitation of the $b^3\Sigma_u^+$ state of H_2 .

Impact energy	Cartwright and Kuppermann (Ref. 7) (OR)	Chung <i>et al.</i> (Ref. 8) (BR)	Rescigno <i>et al.</i> (Ref. 9) (DW)	Integral cross sections (10^{-18} cm ²)			Hall and Andric (Ref. 3) (Expt.)	Nishimura (Ref. 5) (Expt.)	Present (Expt.)
				Fliflet and McKoy (Ref. 10) (DW)	Chung and Lin (Ref. 11) (CC)	Lima <i>et al.</i> (Ref. 13) (CC) ^a			
9	4.40								
10	1.58	17.6							
10.5						28.6	39.0		
11				35.0		41.8	46.0		
11.6							51.5		
12	4.84			62.2		52.5	54.0		
13	5.37	44.7	82.0	78.5	21.9	59.3		54.8	
14	5.45		92.4			62.2			
15	5.27	41.8	88.0	83.0	28.0	61.8		60.4	
16			84.4	80.3	28.4	60.2			
17			74.4					53.7	
18				68.1		54.7			
20	3.56	26.9	54.9	57.8	25.3	47.7		48.4	49.3
25	2.42			31.6	18.2	32.6			
30		11.0		19.6	12.6	21.2		21.2	13.5
35									
40		5.25		8.17	6.22			8.21	7.71
50		2.87		4.02					
60				2.37				3.80	
100		0.40							0.73

^aThe results of Refs. 14 and 15 are in good agreement with those of Ref. 13.

program generally determined the Franck-Condon fitting parameter in approximately five iterations.

A. Differential cross sections

The absolute DCS for the $X \rightarrow b$ excitation were obtained from the measured inelastic to elastic scattering intensity ratios with the utilization of the elastic DCS measured by Khakoo and Trajmar.⁶ The DCS values are given in Table I together with their associated errors. The "experimental error" is due to fluctuations in the electron- and gas-beam fluxes and to the fitting of the continuum profile (the latter includes computed error from the derived error matrix¹⁹ plus statistical error of the integrated counts under the elastic and $X \rightarrow b$ continuum features). The largest contribution to the experimental error was due to the fitting procedure, i.e., the uncertainty of the fitted parameter which was determined from the error matrix of the nonlinear least squares. The "elastic errors" refers to the error in the H_2 elastic DCS of Ref. 6. The error introduced by the uncertainty in the transmission of the analyzer was taken at 10% based on the checks on the $1^1S \rightarrow 2^1P$ transition in He. The total error is the square root of the sum of the squares of the contributing errors.

Figures 2–4 show comparisons of experimental and theoretical differential cross sections for the $X \rightarrow b$ excitation process. Previously, measurements were carried out by Trajmar *et al.*⁴ and Nishimura.⁵ The theoretical re-

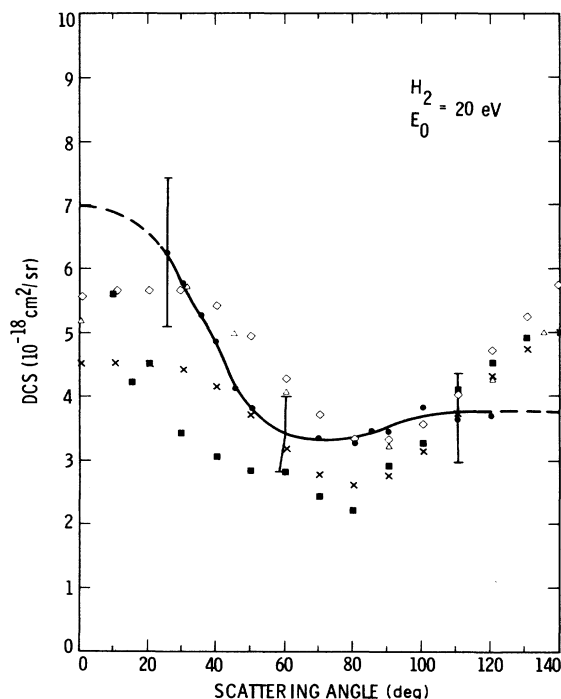


FIG. 2. Comparison of experimental and theoretical DCS for the electron-impact excitation of the $X \rightarrow b$ transition in H_2 . Experiments: ■, Nishimura (Ref. 5); ○ (connected by solid line), present measurements. Theory: △, Rescigno *et al.* (Ref. 9) (DW); ◇, Fliflet and McKoy (Ref. 10) (DW); ×, Lima *et al.* (Ref. 13) (CC). Impact energy is 20 eV.

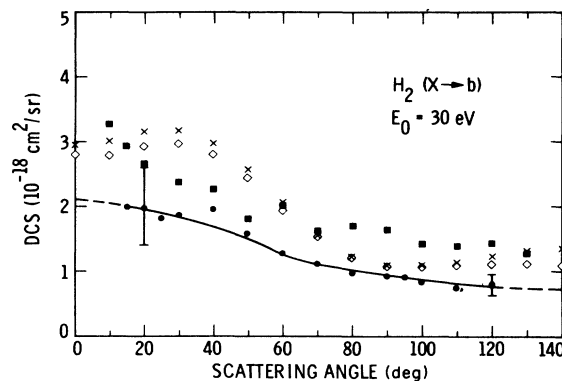


FIG. 3. Same as Fig. 2. Impact energy is 30 eV.

sults include Ochkur-Rudge (OR) calculations from Trajmar *et al.*,⁴ distorted-wave (DW) calculations from Rescigno *et al.*⁹ and Fliflet and McKoy,¹⁰ and two-state close-coupling (CC) calculations from Weatherford¹² and Lima *et al.*¹³ (The cross-section values of Baluja *et al.*¹⁴ and Schneider and Collins¹⁵ are in good agreement with those of Lima *et al.*)

At 20- and 30-eV impact energies, the calculated and experimental cross sections agree reasonably well in shape but differ in magnitude in some cases by about a factor of 2. The experimental results indicate an increase in the DCS at very low scattering angles while the theoretical curves are rather flat in this region. At 40-eV impact energy the experimental data are in good agreement except at low angles but even there they agree within the combined error limits. The various theories^{4,10,12} predict DCS angular distributions which resemble closely the experimental ones and also agree in magnitude with experiment except for the results of Weatherford which are considerably smaller. No theoretical DCS are available at 100 eV.

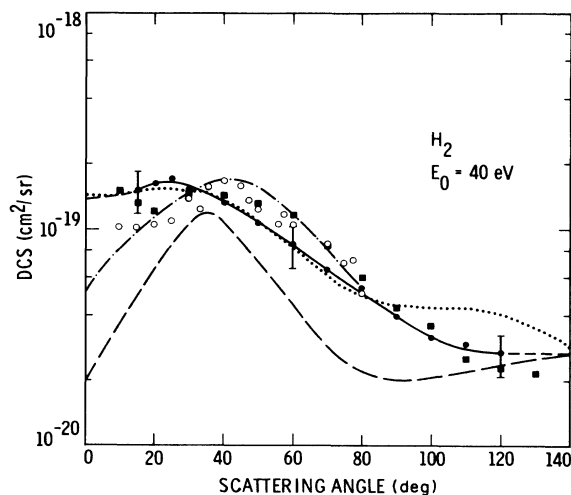


FIG. 4. Same as Fig. 2 except: ○, Trajmar *et al.* (Ref. 4) (expt. normalized to theory); — — —, Weatherford (Ref. 12); · · · · ·, Fliflet and McKoy (Ref. 10); — · — · —, Trajmar *et al.* (Ref. 4) (OR). Impact energy is 40 eV.

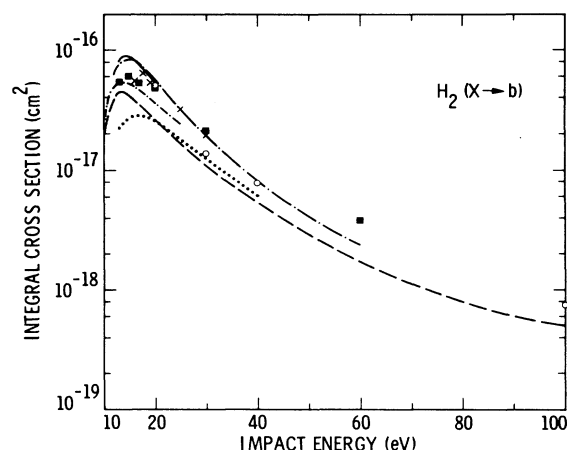


FIG. 5. Comparison of integral cross sections. Theory: —, Rescigno *et al.* (Ref. 9) (DW); — · —, Fliflet and McKoy (Ref. 10) (DW); — — —, Chung *et al.* (Ref. 8) (Born-Rudge); · · · ·, Chung and Lin (Ref. 11) (CC); ×, Lima *et al.* (Ref. 13) (CC); - · - ·, Cartwright and Kuppermann (Ref. 7) (OR). Experiments: ■, Nishimura (Ref. 5); ○, present results.

B. Integral cross sections

Table II summarizes the available integral cross sections. The second column represents Ochkur-Rudge (OR), the third column Born-Rudge (BR), the fourth and fifth columns distorted-wave (DW), and the sixth and seventh columns close-coupling (CC) calculations. The present experimental results are given in the eighth column. For convenience in comparing these cross sections, the results are shown in Fig. 5. The theoretical calculations all predict the maximum in the integral cross section between 14 and 16 eV. However, they differ significantly concerning the magnitude of the cross sections. The experimental data are in close agreement with the two-state close-coupling results of Lima *et al.*¹³ (and Baluja *et al.*¹⁴ and Schneider and Collins¹⁵).

The errors associated with the present integral cross

TABLE III. Dissociation cross sections for H₂.

E_0 (eV)	Corrigan (Ref. 1)	Buckman and Phelps (Ref. 22)	Present ^a
20	0.83	0.58	0.74
30	0.47	0.23	0.22
40	0.26	0.11	0.11
60	0.095	0.024	(0.031) ^b

^aObtained as the sum of the integral cross sections for the $a^3\Sigma_g^+$, $b^3\Sigma_u^+$, and $c^3\Pi_u$ excitations (present value for b and Ref. 23 for a and c).

^bFor the $b^3\Sigma_u^+$ cross section, interpolated value was used.

sections are the same as given in Table I for the DCS. Errors due to extrapolation to unmeasured angles are estimated to be small compared to other errors and can be neglected.

Dissociation cross sections for H₂, which are equal to the sum of integral triplet-state excitation cross sections have been deduced by Buckman and Phelps²² from measurements using electron drift tube technique. They find that the results of Corrigan are not compatible with their measurements. These results and the dissociation cross sections obtained from the present $b^3\Sigma_u^+$ and the $a^3\Sigma_g^+$ and $c^3\Pi_u$ cross sections of Khakoo and Trajmar²³ are summarized in Table III.

ACKNOWLEDGMENTS

The research described in this paper was carried out at the Jet Propulsion Laboratory, California Institute of Technology, and was supported by the National Science Foundation and the National Aeronautics and Space Administration. We would like to express our gratitude to D. C. Cartwright, T. L. Gibson, and V. McKoy for valuable discussions, to H. Nishimura for making available to us his results prior to publication, and to T. Antoni for his help in the measurements and data evaluation.

*Present address: Department of Physics, University of Windsor, Windsor, Ontario, Canada.

†Present address: Department of Physics, The Queen's University of Belfast, Belfast BT7 1NN, Northern Ireland.

‡Permanent address: Space Physics Research Laboratory, University of Michigan, Ann Arbor, Michigan 48105.

¹S. J. B. Corrigan, *J. Chem. Phys.* **43**, 4381 (1965).

²A. Weingartshofer, H. Ehrhardt, V. Hermann, and F. Linder, *Phys. Rev. A* **2**, 294 (1970).

³R. I. Hall and L. Andric, *J. Phys. B* **17**, 3815 (1984).

⁴S. Trajmar, D. C. Cartwright, J. K. Rice, R. T. Brinkmann, and A. Kuppermann, *J. Chem. Phys.* **49**, 5464 (1968).

⁵H. Nishimura, *J. Phys. Soc. Jpn.* **55**, 3031 (1986); and (private communication).

⁶M. A. Khakoo and S. Trajmar, *Phys. Rev. A* **34**, 138 (1986).

⁷D. C. Cartwright and A. Kuppermann, *Phys. Rev.* **163**, 861 (1967).

⁸S. Chung, C. C. Lin, and T. P. Lee, *Phys. Rev. A* **12**, 1340 (1975).

⁹T. N. Rescigno, C. W. McCurdy, and V. McKoy, *Phys. Rev. A* **13**, 216 (1976).

¹⁰A. W. Fliflet and V. McKoy, *Phys. Rev. A* **21**, 1863 (1980).

¹¹S. Chung and C. C. Lin, *Phys. Rev. A* **17**, 1874 (1978).

¹²C. A. Weatherford, *Phys. Rev. A* **22**, 2519 (1980).

¹³M. A. P. Lima, T. L. Gibson, W. Huo, and V. McKoy, *J. Phys. B* **18**, L865 (1985); and (private communication).

¹⁴K. L. Baluja, C. J. Noble, and J. Tennyson, *J. Phys. B* **18**, L851 (1985).

¹⁵B. I. Schneider and L. A. Collins, *J. Phys. B* **18**, L857 (1985).

¹⁶A. Chutjian, *J. Chem. Phys.* **61**, 4279 (1974).

¹⁷D. G. Truhlar, J. K. Rice, A. Kuppermann, S. Trajmar, and D. C. Cartwright, *Phys. Rev. A* **1**, 778 (1970); R. I. Hall, G. Joyez, J. Mazeau, J. Reinhardt, and C. Schermann, *J. Phys. (Paris)* **34**, 827 (1973).

- ¹⁸D. F. Register, S. Trajmar, and S. K. Srivastava, *Phys. Rev. A* **21**, 1134 (1980).
- ¹⁹P. R. Bevington, *Data Reduction and Error Analysis for the Physical Sciences* (McGraw-Hill, New York, 1969), pp. 215–219.
- ²⁰T. L. Gibson (private communication).
- ²¹W. Kolos and L. Wolniewicz, *J. Chem. Phys.* **43**, 2429 (1965).
- ²²S. J. Buckman and A. V. Phelps, *J. Chem. Phys.* **82**, 4999 (1985).
- ²³M. A. Khakoo and S. Trajmar, *Phys. Rev. A* **34**, 146 (1986).